Available online at www.sciencedirect.com
SCIENCE DIRECT®

Journal of the European Ceramic Society 24 (2004) 739–752

www.elsevier.com/locate/jeurceramsoc

Processing of barium titanate tapes with different binders for MLCC applications—Part I: Optimization using design of experiments

Dang-Hyok Yoon, Burtrand I. Lee*

School of Materials Science and Engineering, Olin Hall, 340971, Clemson University, Clemson, SC 29634-0971, USA

Received 28 October 2002; received in revised form 20 April 2003; accepted 27 April 2003

Abstract

Twenty-four kinds of $BaTiO_3$ slips for MLCC application were investigated using three different binder systems: one solvent-based, and two water-based with water-soluble acrylic binder and aqueous emulsion binder systems. The half-fractional factorial design method was used for each system with four input factors with two levels for each factor. Tape casting, K-square preparation, sintering and characterization were conducted. Slip viscosity, mechanical properties of the green tapes, green and sintered density of K-squares, and dielectric permittivity were analyzed as output responses using statistical analysis methods. Most of the green body properties from solvent-based system such as tensile strength, tape morphology and bulk density depended on the ceramic powder. While, dispersant was the most significant factor for the two water-based systems. The sintered properties such as microstructure and dielectric permittivity for the three systems depended significantly on the type of ceramic powder. Finally, an optimization was performed for each system by means of a scorecard which was used to prioritize all samples to important output responses through the numerical ranking method.

Keywords: $BaTiO_3$; Design of experiments; Dielectric properties; Tape casting

1. Introduction

A multilayer ceramic capacitor (MLCC) has alternating layers of dielectric materials and internal metal electrodes. Currently, production of commercial MLCCs of two to three micrometers-thick green ceramic sheets containing several hundred layers yields the highest volumetric efficiency.[1] During MLCC production process, a mixture of ceramic powder and binder solution is formed into green ceramic sheets by tape casting. Subsequent steps include screen printing of the internal electrode on the green sheet, stacking to obtain the desired number of layers, laminating, cutting, binder burn-out, sintering, etc. Therefore, experiment on MLCC usually involves a number of input factors as well as many output responses, all of which are correlated with one another. In addition, planning such a study and analyzing the experimental results require the knowledge of many different fields, including powder characterization, slip behavior, tape casting, the interaction between metal and dielectrics, binder burn-out and sintering behavior.

The traditional experimental method, one-factor-at-a-time approach, can hardly be used to establish relationships among all the experimental input factors and the output responses for such a complex system. Even though the traditional approach can be useful in finding predominant factors in this situation, it is time- and energy-consuming method. Furthermore, since the results are valid only under fixed experimental conditions, prediction based on them for other conditions is uncertain.[2] Design of experiments (DOE), on the other hand, is a very powerful tool which can be used to optimize designs for performance, quality, and cost having many different input variables. DOE is a process of testing using a structured plan in which the input factors are varied in an organized manner to optimize efficiently output responses of interest with minimal variability. Due to the statistical balances in the design, number of potential combinations of numerous input factors at different levels can be evaluated for the best overall combination, in a small number of experiments.[3]

* Corresponding author. Tel.: +1-864-656-5348; fax: +1-864-565-1453.
E-mail address: burt.lee@ces.clemson.edu (B.I. Lee).

0955-2219/03/$ - see front matter © 2003 Elsevier Ltd. All rights reserved.
doi:10.1016/S0955-2219(03)00333-9

The subsequent interpretation of the resulting experimental data based on analysis of variance (ANOVA) will identify the input factors that influence the results the most and those that do not, and the presence of interactions among the input factors. The following step is optimization which leads to the best possible output response by choosing adequate levels of input factors. Because most of us can only grasp the effect of one-factor-at-a-time in our minds, we need mathematics and computer to keep track of the factors and their combinations in DOE.

The aim of this work presented in a series of two papers is to investigate $BaTiO_3$ slip systems made from three different kinds of binders: one solvent-based and two water-based. Half-fractional factorial designs were performed separately for each binder system, i.e. three sets of experiments, using four input factors with two levels for each input factor. 2^4 or 16 runs of experiment are required for full factorial design, but eight runs for half-fractional factorial design. Fractional factorial designs use a well-balanced subset of the possible combinations of the levels of factors to reduce the time and cost of experiment. This method is particularly recommended when most of the quantities of interest can still be estimated from the smaller number of experiment. With this design, we are still able to estimate the overall mean and the main effects of the factors.[2] MINITAB, statistical and graphical analysis software, was used for the experimental table generation and analysis of the results. Slip viscosity, tensile strength of green tapes, green and sintered density of small rectangular-shaped K-squares, and dielectric permittivity were analyzed as output responses. In Part I, the effect of each input factor on output responses and optimization for three different slip systems are described by means of ANOVA, main effects plot, and scorecard. In Part II, physical properties of three different systems will be compared using a graphical method.

2. Experimental procedure

Table 1 presents eight runs of the half-fractional factorial design for three different binder systems each, hence 24 runs as a whole, statistically chosen by MINITAB. Binder type was the controlled factor, and dispersant was the fixed one for solvent-based system, while the opposite was true for two water-based systems. In addition, factor levels for liquid medium to binder resin ratio and binder amount for aqueous

Table 1
Eight runs of design for three different binder systems using four input factors with two levels for each factor selected by MINITAB

Run	Sample name	Input factors					
		Binder	Dispersant	Solvent/resin ratio	Water/resin ratio	Binder amount (wt.%)	Powder
(a) Solvent-based binder system							
1	S1	B-98		8/1		8	BT-8
2	S2	B-76		8/1		8	BT219-6
3	S3	B-98		10/1		8	BT219-6
4	S4	B-76		10/1		8	BT-8
5	S5	B-98		8/1		10	BT219-6
6	S6	B-76		8/1		10	BT-8
7	S7	B-98		10/1		10	BT-8
8	S8	B-76		10/1		10	BT219-6
(b) Water-soluble acrylic binder system							
1	W1		m-PMMA		8/1	8	BT-8
2	W2		APA		8/1	8	BT219-6
3	W3		m-PMMA		10/1	8	BT219-6
4	W4		APA		10/1	8	BT-8
5	W5		m-PMMA		8/1	10	BT219-6
6	W6		APA		8/1	10	BT-8
7	W7		m-PMMA		10/1	10	BT-8
8	W8		APA		10/1	10	BT219-6
(c) Aqueous emulsion binder system							
1	E1		PApA-Na		6/1	10	BT-8
2	E2		APA		6/1	10	BT219-6
3	E3		PApA-Na		8/1	10	BT219-6
4	E4		APA		8/1	10	BT-8
5	E5		PApA-Na		6/1	12	BT219-6
6	E6		APA		6/1	12	BT-8
7	E7		PApA-Na		8/1	12	BT-8
8	E8		APA		8/1	12	BT219-6

emulsion binder system had to be changed from the other two systems due to the low slip viscosity of the emulsion system.

Two kinds of $BaTiO_3$ powders were used as the ceramic phase for all systems to understand the influence of the powder: one was hydrothermally prepared BT-8 (Cabot Performance Materials, Boyertown, PA) with a mean particle size of 0.24 μm and a specific surface area of 8.50 m^2/g, and the other was solid-state high temperature reacted BT 219-6 (Ferro Electronic Materials, Penn Yan, NY) with a mean particle size of 1.38 μm and a specific surface area of 2.84 m^2/g. Both powder morphologies are shown in Fig. 1.

Commercial polyvinyl butyral (PVB) resins, B-98 and B-76, (Solutia, St. Louis, MO) with different molecular weights were used for the solvent-based binder phase. More detailed description on the PVB resin can be found in the literature.[4,5] To prepare the solvent-based binder solution, 30 g of PVB polymer resin was dissolved in a 60/40 (wt.%) toluene/ethanol mixture. Then, 40 wt.% of dioctyl phthalate with respect to the weight of PVB resin was added as a plasticizer. The mixture was stirred for 12 h at an ambient condition. Total solvent to polymer resin ratio was fixed at 8/1 or 10/1. A proprietary acrylic formulation binder solution (WB40B, Polymer Innovations, San Marcos, CA) with the viscosity of 9200 mPa s was used as the water-soluble acrylic binder phase. According to the supplier's data,[6] it already contained acrylic resin (19.2 wt.%), plasticizer (4.2 wt.%), and defoamer (0.46 wt.%) in water. Based on our pre-test results, the plasticizer amount in the binder system was increased to 40 wt.% with respect to the acrylic resin by adding more of the same plasticizer (PL001, Polymer Innovations, San Marcos, CA) to achieve enough flexibility of the final green tape. An acrylic emulsion (Duramax B-1070, Rohm and Haas Co., Philadelphia, PA) with 44 wt.% solids content was used as binder phase for aqueous emulsion system. A 20 wt.% of PL001 plasticizer with respect to the solid resin was added in this system.

Eight different kinds of ceramic slips for each system, as shown in Table 1, were prepared in a multi-step process. First, 60 g of $BaTiO_3$ powder was added to the

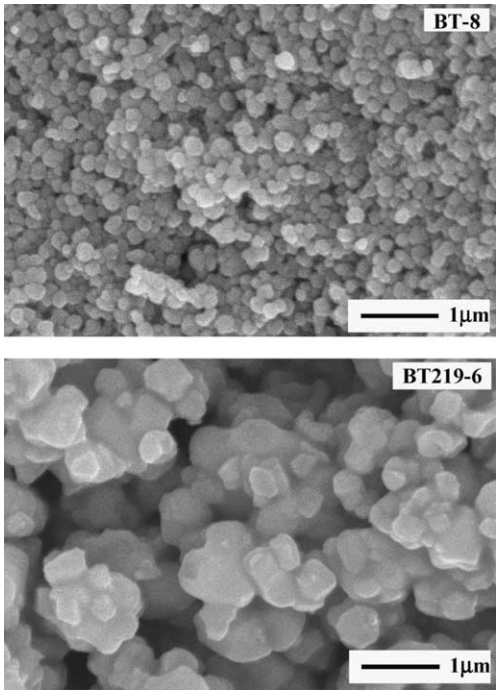

Fig. 1. SEM micrographs of BT-8 and BT 219-6 starting ceramic powders.

Table 2
Materials information

Material	Name	Description
Solvent-based binder system		
PVB resin	B-98	MW = 55,000, T_g = 75 °C
	B-76	MW = 105,000, T_g = 66 °C
Dispersant	m-PMMA	Modified polymethylmethacrylate, MW = 35,000
Solvent		Toluene/Ethanol = 60/40 wt.%
Plasticizer		Dioctyl phthalate
Water-soluble acrylic binder system		
Binder solution	WB40B	Formulated acrylic binder T_g = 40 °C, resin MW = 100,000
Dispersant	m-PMMA	Modified polymethylmethacrylate, MW = 35,000
	APA	ammonium salt of polyacrylic acid, MW = 6000
Plasticizer	PL001	polyether polyol
Surfactant	S465	tetramethyldecynediol + ethylene oxide
Defoamer	DF001	modified silicone copolymer
Aqueous emulsion binder system		
Binder solution	B-1070	acrylic emulsion, pH = 6.2, T_g = −6 °C
Dispersant	PApA-Na	sodium salt of polyaspartic acid, MW = 4500
	APA	ammonium salt of polyacrylic acid, MW = 6000
Plasticizer	PL001	polyether polyol
Surfactant	S465	tetramethyldecynediol + ethylene oxide
Defoamer	DF001	modified silicone copolymer

binder solution which was pre-weighed to be 8, 10 or 12 wt.% of binder resin with respect to the ceramic powder. The binder solutions already contained a certain amount of dispersant which was 0.3 wt.% in solvent-based and water-soluble binder system, and 0.5 wt.% in emulsion system. Second, surfactant (S465, Air Products and Chemicals, Allentown, PA) was added to decrease the surface tension of water. According to the supplier's data, 73.05 dynes/cm of water surface tension can be decreased to 41.9 dynes/cm by adding 0.1 wt.% of S465 surfactant. Third, 0.2 wt.% of defoamer (DF001, Polymer Innovations, San Marcos, CA) with respect to the total slip was added. These surfactant and defoamer were only needed for the water-based systems due to the high surface tension and easy tendency for foaming. Fourth, pH of the water-based slips were adjusted to 9.7 ± 0.1 by adding ammonium hydroxide to stabilize the binder solution and to control the Ba^{2+} ion leaching in water.[7] Fifth, the slips were ball-milled with 400 g of cylindrical-shaped yittria-stabilized zirconia media for 24 h. All of the materials used are listed in Table 2.

Some steps had to be changed for emulsion system because of the unique nature of this system. Since an emulsion is a dispersion of insoluble polymer particles stabilized by an anionic surfactant in water, ball-milling energy was found to damage the emulsion stability. Therefore, the binder solution was mixed by moderate stirring after the first-stage ball-milling without binder phase which was performed to disperse the ceramic powder in water. The samples E1 and E7 among eight slips with emulsion binder, prepared with the combination of PApA-Na and BT-8, gelled during slip preparation, which were not able to carry on to further process.

To remove any residual air bubbles and to stabilize the slip, 10 rpm slow rolling for 24 h without the media was performed. The rheological behavior of the slips was characterized using a programmable rheometer (model DV-III, Brookfield, Stoughton, MA). The measurements utilized a small sample adapter and a SC4-21 spindle at a constant temperature of 25 °C in the shear rate range of 1–140 s^{-1} in ascending and descending order.

Tape casting was done for all slips, except for E1 and E7, using a table top tape caster (TTC-1000, Richard E. Mistler, Morrisville, PA) with a 4-inch wide single doctor blade on moving polypropylene film. The casting rate was 20–50 cm/min, and the tapes were dried in the drying zone of the tape caster at an air flow temperature of 90–100 °C depending on binder system. After gold coating, the green microstructure of tapes was observed using a scanning electron microscope (SEM; Hitachi S-3500N).

To make a K-square, the green tapes were cut (8.0×8.0 cm^2) and stacked into the thickness of approximately 1 mm. This stacked bar was laminated at a pressure of 300 kPa for 5 min at 80–120 °C using a programmable press machine (model 3891, Carver Inc., Wabash, IN) and then cut into small rectangular-shaped K-squares (2.0×1.8 cm^2). The green density of K-squares was determined by using a geometrical method with at least six samples per each condition. The thickness and length were measured using a micrometer accurate to 0.001 mm and the weight was measured using a scale accurate to 0.1 mg.

Mechanical property testing of the green tapes was performed using a tensile tester (Minimat 2000, Rheometric Scentific, Piscataway, NJ) with a 200 N load cell. Dumb-bell shaped specimens with 3 mm width and 10 mm length were cut from the green tapes toward casting

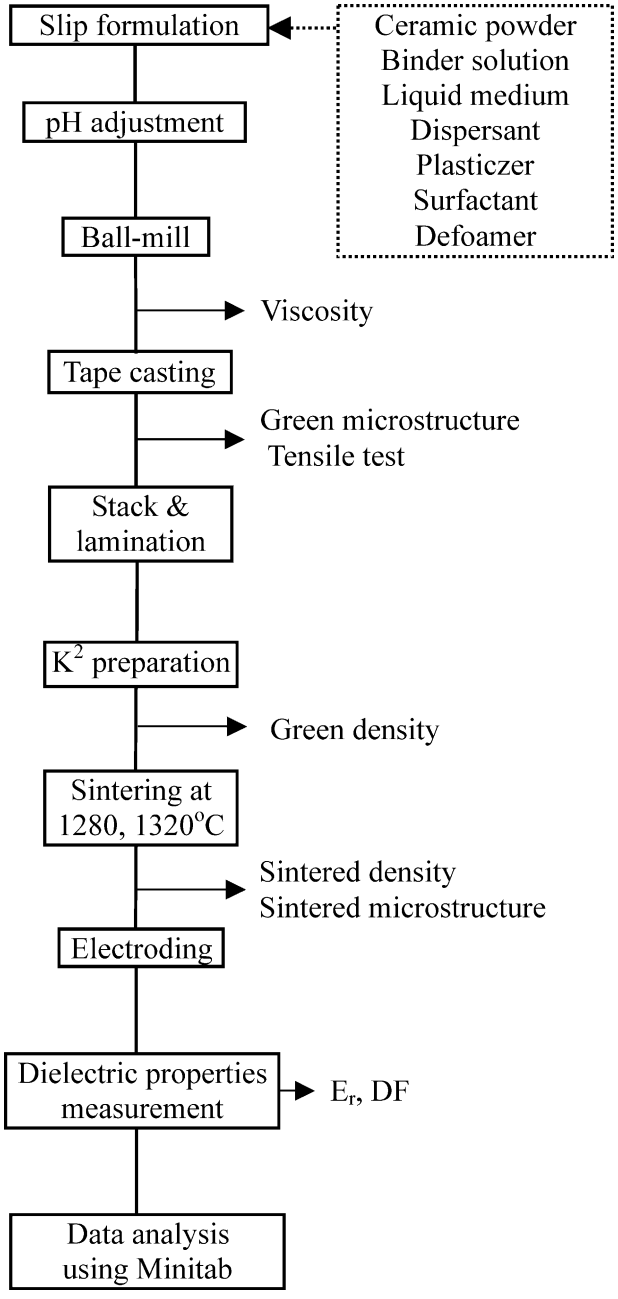

Fig. 2. Schematic experimental procedure for $BaTiO_3$ slip systems.

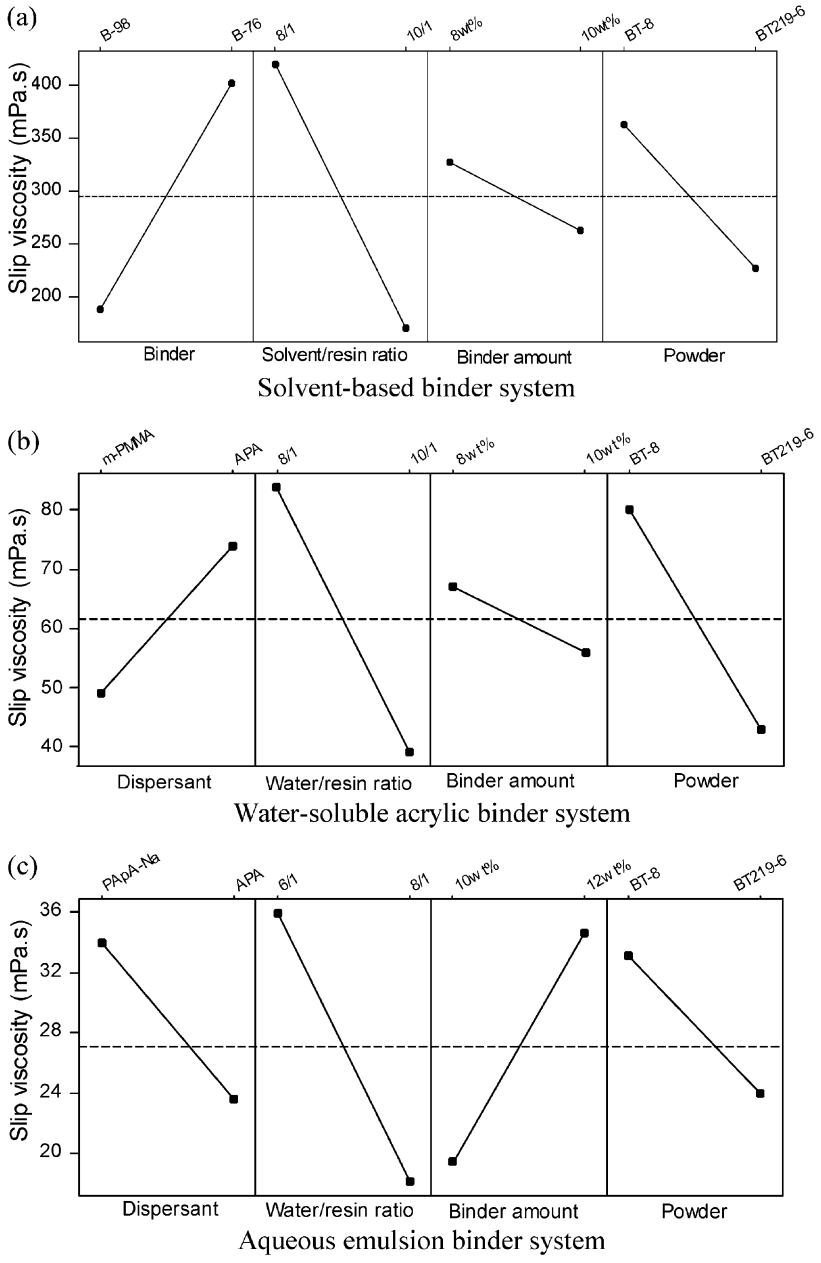

Fig. 3. Main effects plot of slip viscosity for three different binder systems.

direction using a sample cutter. The tensile tests were performed at ambient temperature of 22 ± 1 °C with the rate of 1 mm/min. At least five samples were tested to calculate the average tensile properties of these tapes. A Windows-supported software was used to control the instrument and to gather the stress and strain data.

Four K-square samples for each condition were sintered at 1280 and 1320 °C for 2 h in air with a heating and cooling rate of 3 °C/min. The sintered density was measured using the geometric method. Three of the four samples for each condition were electroded with silver paste and then fired at 550 °C for 12 min to burn-out the polymeric species in the metal paste. After gold coating, the sintered microstructure of the K-square surface was examined under SEM. The capacitance and the dissipation factor were measured at 1 kHz/1 V_{rms}, using a HP 4284A LCR meter after stabilizing the K-squares for 6 h after electrode firing.

Every experimental step in this study was made to keep systems as similar as possible to each other for a fair comparison. However, additional steps such as surfactant and defoamer addition, and pH adjustment were required for water-based systems. In addition, the casting conditions such as casting rate, drying temperature, and lamination temperature were adjusted due to the different liquid medium and binder. The schematic of the experimental procedure is given in Fig. 2.

3. Results and discussion

3.1. Slip properties

Fig. 3 shows the main effects plot of slip viscosity for the three systems, the points in the graph being the means of the slip viscosity at two levels of each input factor. A dashed reference line is drawn at the grand mean of the viscosity data. The plot indicates that the lower solvent/resin ratio and a fine BT-8 ceramic powder increase the slip viscosity. The effect of ceramic powder is attributed to the higher specific surface area of BT-8 compared with BT 219-6.

For the effect of binder resin of solvent-based system in Fig. 3(a), slips with larger molecular weight of resin (B-76) show the higher viscosity. The number of B-76 molecules in the slip is only a half of B-98 for a weight-based addition since B-76 has almost twice the molecular weight of B-98. Therefore, we can conclude that the role of chain length is more important than the number of polymer molecules on the viscosity in this case.

One of the significant factors for water-soluble binder system is the dispersant, showing lower viscosity with modified-PMMA (m-PMMA) than APA as shown in Fig. 3(b). This means more efficient powder dispersion with m-PMMA. According to the manufacturers, m-PMMA has been modified from polymethylmethacrylate (PMMA) having polymethacrylate/polyacrylic acid backbone with polyethylene glycol (PEG) side chains. Therefore, it is an anionic dispersant in water with multi-functionalities which has a totally different characteristics from a non-ionic PMMA. The differences in functional group and hydrodynamic radius[8] originated from the molecular weight between m-PMMA (MW = 35,000 g/mol) and APA (MW = 6000 g/mol) contribute to this viscosity behavior.

On the other hand, APA is an efficient dispersant for the emulsion system as shown in Fig. 3(c). However, the effects of dispersant and ceramic powder for emulsion system should not be over trusted because of the missing data of E1 and E7. The missing data introduce a problem into the analysis since experimental treatments are no longer orthogonal. Even though there are general approaches to the missing data problem such as an estimation of the missing values,[3] it will not be considered here because it is beyond of the scope of this work. As an alternative, we will draw a general conclusion based on the experimental results for the emulsion system.

It is generally believed that the lower slip viscosity means better dispersion for the slips containing the same amount of solids, which is more favorable for producing thinner ceramic tapes for MLCC application. If one of thin MLCC layers contains small air pockets or pores which originate from poor powder dispersion, failure of the final products may result. Therefore, a well-dispersed slip is very important to ensure the long-term stability and quality of the final products.

3.2. Green body properties

The green density of K-squares for three different systems is presented in Fig. 4 using a box plot. Although the geometrical measurement method was used to determine the green density of K-squares, the variation within the same sample group was much smaller than the variations between the different groups, meaning this method is reliable. The values are within the range of 3.03 (S2)–3.59 (S1), or 50–59% of the theoretical density of $BaTiO_3$ for the solvent-based system, 3.09 (W8, 51%)–3.87 (W3, 64%) for water-soluble binder system, and 3.00 (E8, 50%)–3.60 (E3, 60%) for emulsion system. High green density is required for a high

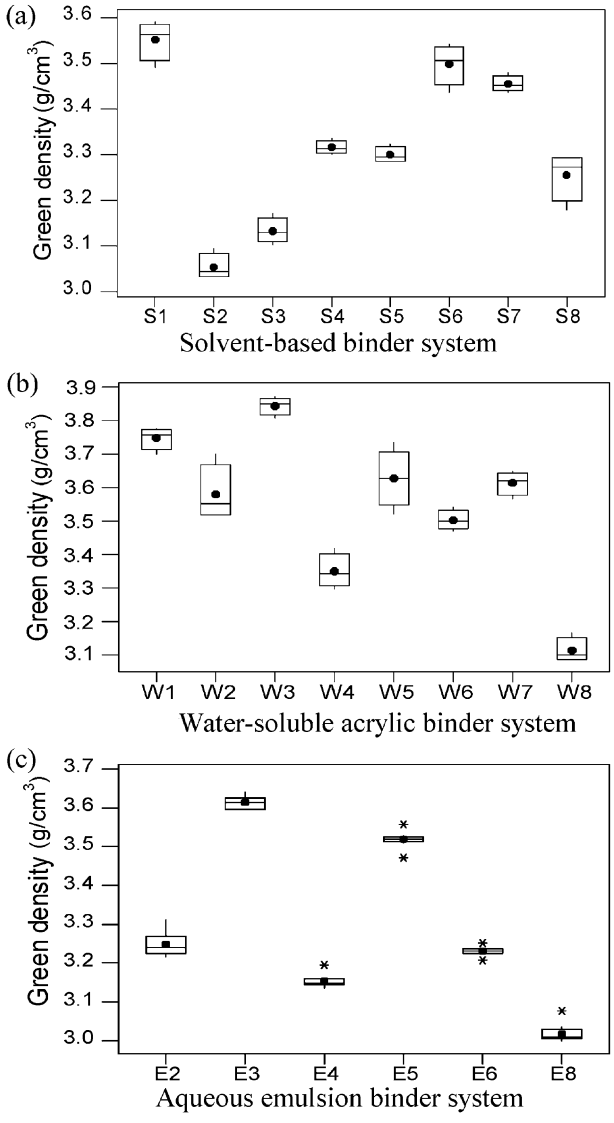

Fig. 4. Green density of K-squares for three different systems.

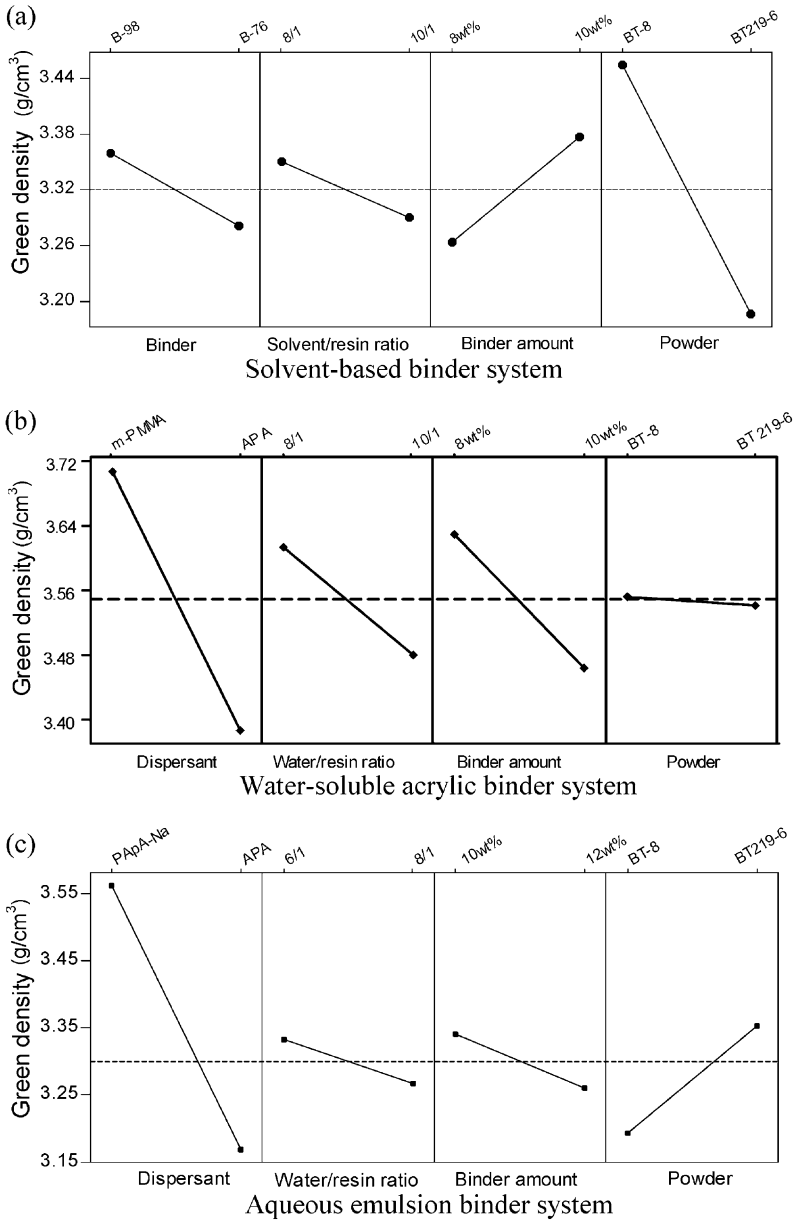

Fig. 5. Main effects plot for the K-square green density of three different systems.

reliability of final MLCC products, especially those with very thin dielectric layers.

The main effects of the input factors on the green density of the K-squares are displayed in Fig. 5. As shown in Fig. 5(a), powder is the only significant factor for solvent-based system according to the statistical analysis with 95% confidence level. It shows higher density with K-squares made from BT-8 than those from BT 219-6. To achieve high particle packing, the powder must have a small spherical shape,[9,10] though the large specific surface area of small powder makes the powder difficult to handle because of the high tendency for agglomeration. The green density difference of the solvent-based system shown in Fig. 5(a) can be explained in terms of the particle shape and size distribution of the powders shown in Fig. 1.

On the other hand, dispersant is the most significant factor for the two water-based systems in Fig. 5(b) and (c). K-squares with m-PMMA dispersant show much higher green density than those with APA in the water-soluble system, while PApA-Na is more effective than APA for the emulsion system. The lower slip viscosity with m-PMMA for water-soluble system results in higher green density, but not with APA for emulsion system. The explanation for the difference will be given in conjunction with green microstructure later. The dispersion of water-based system is more complicated than solvent-based system because of two different operating mechanisms: electrostatic repulsion and steric stabilization.

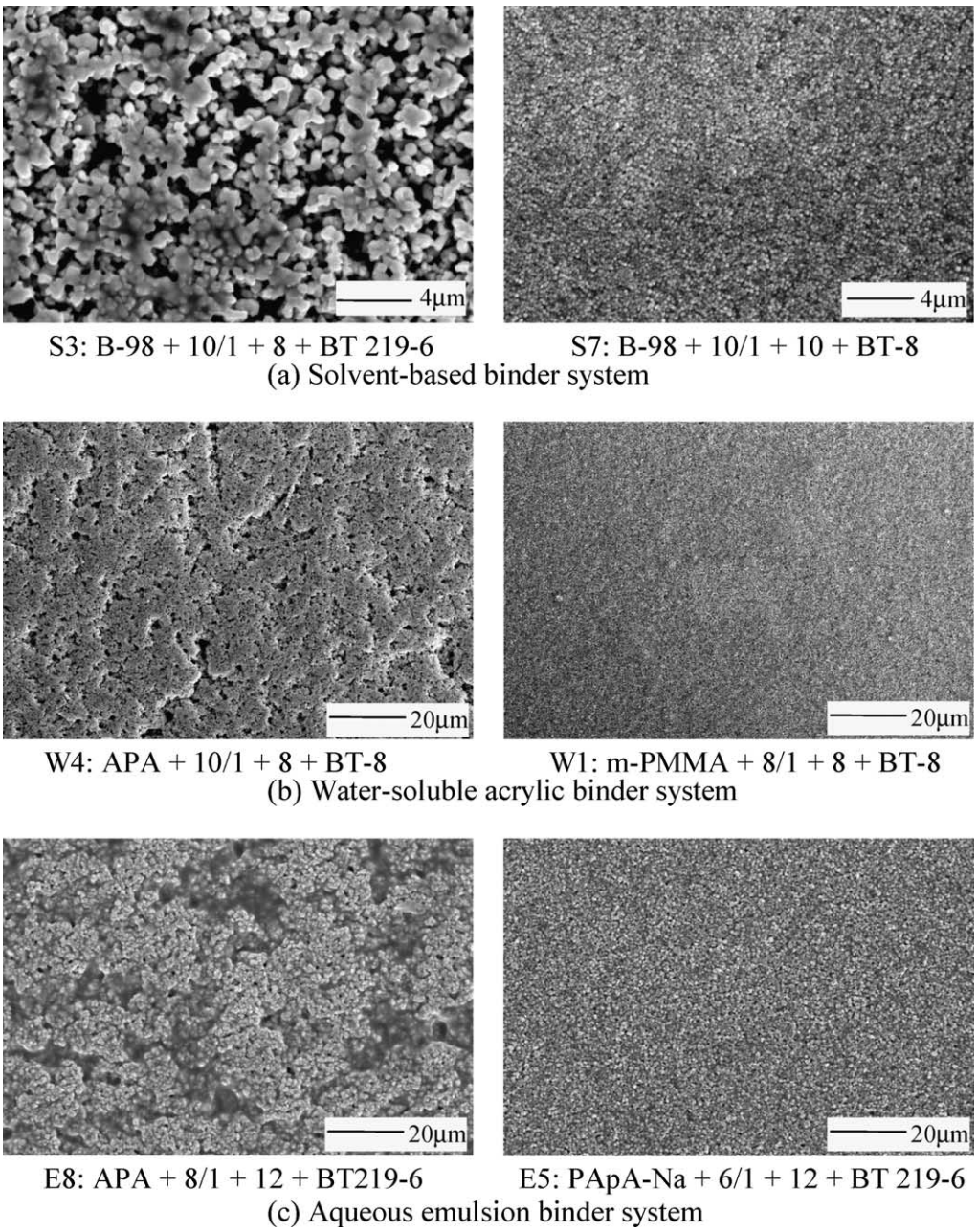

Fig. 6. SEM microstructures of the green tapes made from different binder systems.

Electrostatic repulsion is less effective in solvent-based system because of the lower dielectric constant and ionic concentration of nonaqueous medium.[11]

The characteristic green surface microstructures of cast films are seen in Fig. 6. The solvent-based system in Fig. 6(a) shows that the tapes made from BT-8 have a smooth and well-packed surface morphology, while the tapes made from BT 219-6 show a rough and porous structure. For the water-based systems, dispersant is the most important factor as shown in Fig. 6(b) and (c). Modified PMMA for the water-soluble binder system and PApA-Na for the emulsion system tapes show a smooth and well-packed surface morphology regardless of the ceramic powder used. All these green morphologies agree with the green density behavior of K-squares shown in Fig. 5. In terms of the slip viscosity, emulsion-type slips with APA dispersant exhibits generally lower viscosity than those with PApA-Na in Fig. 3(c). However, the opposite results appear with green density and surface morphology as shown in Figs. 5(c) and 6(c). Therefore, this porous surface morphology with APA dispersant cannot be explained with the poor slip dispersion. This result seems to be related to the interaction between dispersant and binder resin during the drying process. Emulsion remains as a discrete particulates in the slurry, acting as a binder by forming films

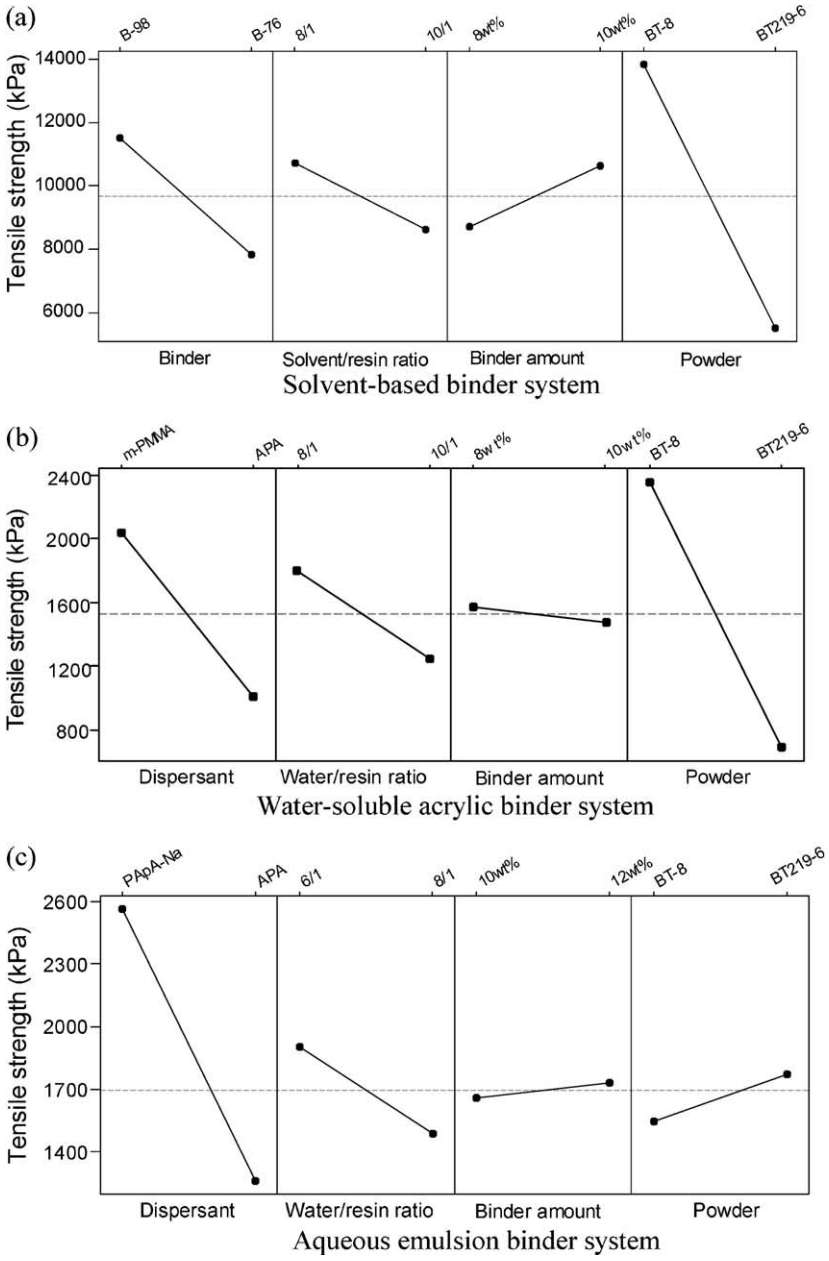

Fig. 7. Main effects plot of the green tapes for the engineering tensile strength.

upon drying when the water phase evaporates. The uniform film formation and shrinkage rate at a certain drying stage is very important to achieve a dense green surface morphology despite the well-dispersed slip. However, the detailed explanation on this result needs further study.

Fig. 7 presents the main effects plots for the engineering tensile strength of three different kinds of green tapes. For the solvent-based system shown in Fig. 7(a), higher mechanical strength of the tapes with B-76 was expected than those with B-98 because of the higher molecular weight. However, the tapes with B-98 ($T_g = 75$ °C) show higher strength than those with B-76 ($T_g = 66$ °C). The T_g of the binders may be considered to explain the result. The green strength of ceramic is known to be affected by T_g of a plasticized binder as well as the cohesive strength of the binder.[12,13] It is also known that the green body strength of pellets with a PVA binder increases as T_g increases.[14] Another possible reason is the number of molecules of binder resin in the slip system as explained previously. However, the effect of powder is more dominant than the binder molecular weight on the engineering tensile strength. With the lower green density and the porous green microstructure of BT 219-6 as shown in Figs. 4(a) and 6(a), the lower strength of the tapes made from BT 219-6 was expected. According to the model proposed by Onoda,[12] strength of ceramic green bodies is correlated

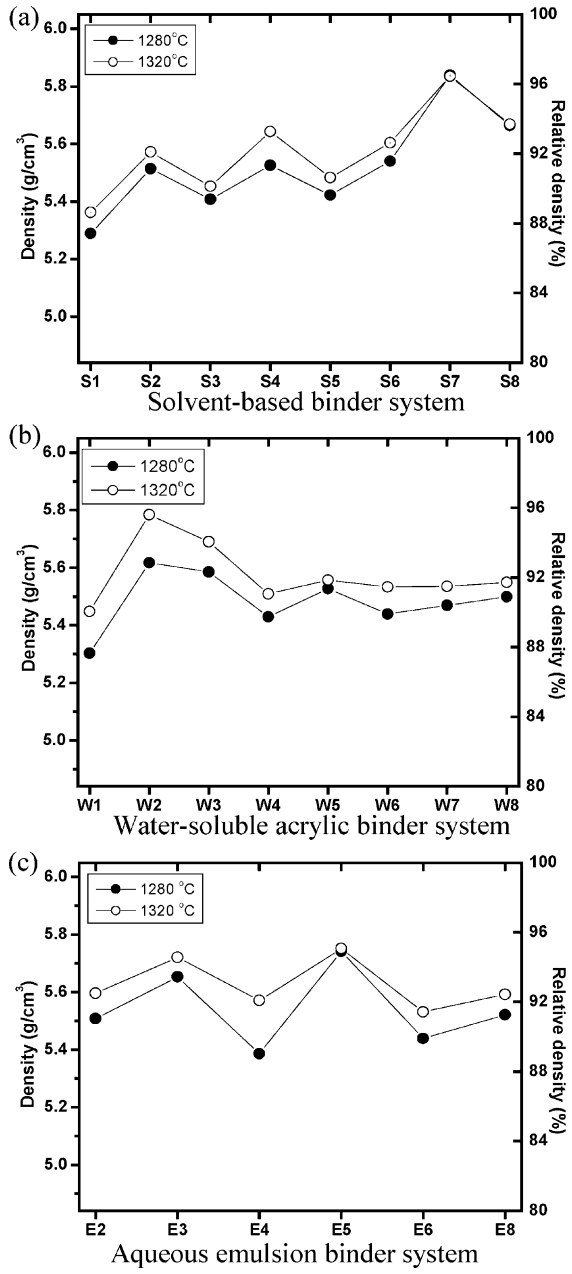

Fig. 8. Sintered density of K-squares at 1280 and 1320 °C.

not only to the cohesive strength and quantities of binder but also the packing density of the particulates. The effects of the solvent/resin ratio and the added binder amount were insignificant.

The significant factors for the water-soluble system in Fig. 7(b) are ceramic powder and dispersant. With the higher green density and the denser green microstructure of the tapes with m-PMMA, the higher strength of these tapes can be explained. Our results show that the average tensile strength of the tapes made from BT-8 with m-PMMA (W1 and W7) is 2890 kPa, while tapes made from BT 219-6 with APA (W2 and W8) was 270 kPa. Dispersant is the only significant factor for the emulsion system as shown in Fig. 7(c). The effect of the ceramic powders cannot be decided due to the two missing data set for BT-8.

3.3. Sintered and dielectric properties

Fig. 8 shows density of the K-square samples sintered at 1280 and 1320 °C in air. Solvent-based system in Fig. 8(a) shows the density values from 5.30 (S1) to 5.84 (S7), or 88–97% of the theoretical density of $BaTiO_3$. Based on the statistical analysis with a 95% confidence level, there is no significant input factor which can affect the sintered density. This means that the sintered density is affected by other factors which are not included in the input factors selected. The sintered density for water soluble system is in the range of 5.30 g/cm^3 (W1, 1280 °C, 88%) to 5.78 g/cm^3 (W2, 1320 °C, 96%), while for emulsion system 5.39 g/cm^3 (E4, 1280 °C, 89%) to 5.75 g/cm^3 (E5, 1320 °C, 95%). According to the statistical results, powder is the most significant factor for two water-based systems, showing much higher density with the K-squares made from BT 219-6. This powder effect may come from the different level of impurities presented in the powder. This will be explained below along with Fig. 9. The effect of dispersant, the most significant factor for the green density, is shown to be relatively small compare to the powder effect. This can be explained that the green microstructure and the green density did not translate into the sintered density during the high temperature sintering. The sintered density is slightly increased by raising the sintering temperature from 1280 to 1320 °C for all systems.

Fig. 9 shows the K-square microstructures of three different systems which were sintered at 1280 and 1320 °C. Even though only four samples are shown here, the following two general features are found for all samples. The first is that samples made from BT 219-6 show higher tendency for abnormal grain growth than those from BT-8, which makes the ceramic powder is the most significant factor on sintered microstructure. The second is that water-based systems show higher tendency for abnormal grain growth than solvent-based one under the same sintering conditions such as temperature and ceramic powder. The different onset temperature for the abnormal grain growth between two powders can be explained with the different levels of trace impurities in them. Most of the commercial undoped $BaTiO_3$ powders contain impurities such as Si, Al or Na between 20 and 100 ppm, especially higher amounts in the solid-state reaction powders due to the inherent weakness of its processing method.[15,16] The presence of these impurities can decrease the eutectic point to lower than 1317 °C which is the eutectic temperature of the $BaO–TiO_2$ system.[17] The small areas with a low melting temperature can act as nuclei for abnormal grain growth. Melted phase can be found in the grain boundaries of BT 219-6 sintered at 1320 °C in

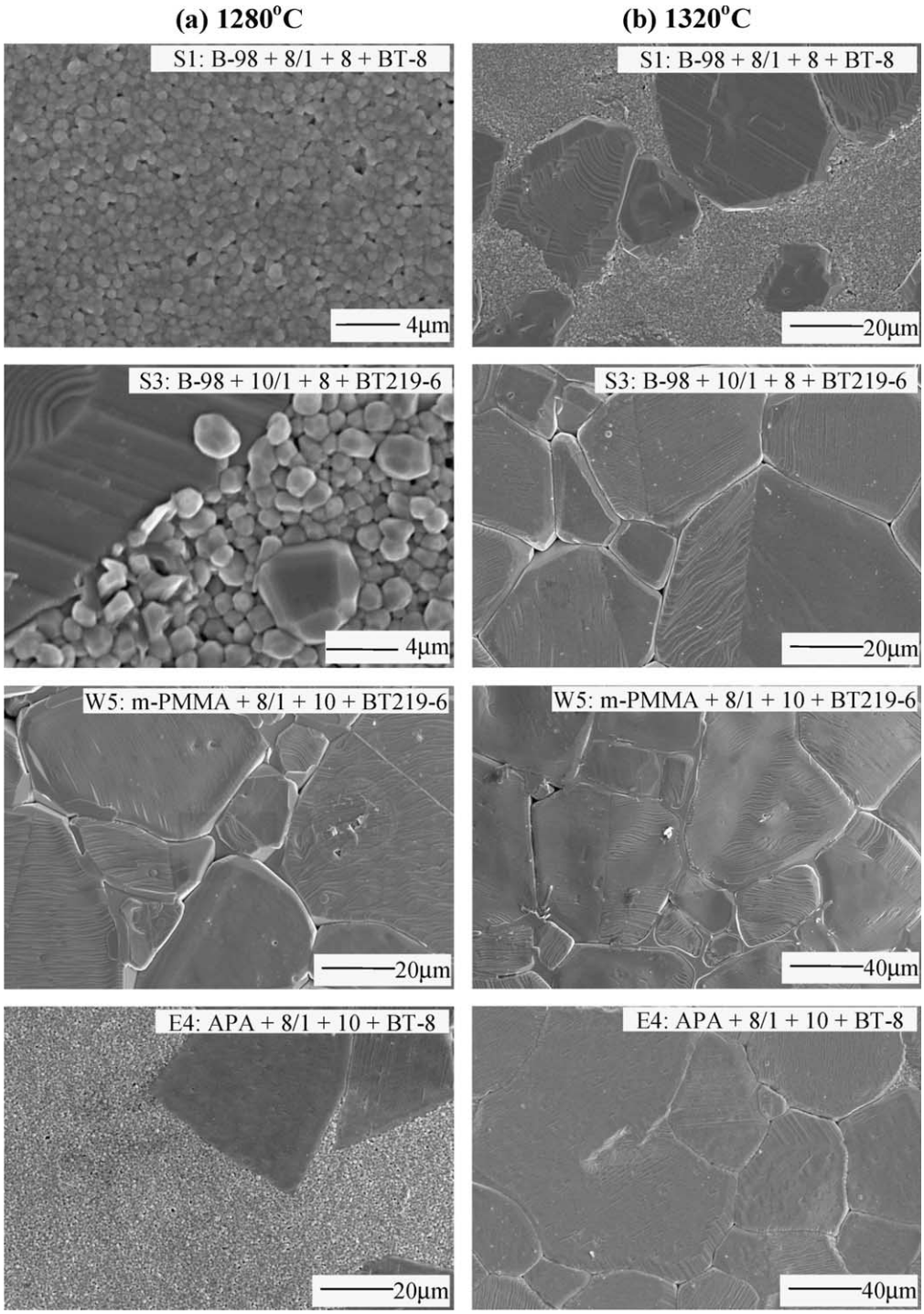

Fig. 9. Schematic microstructure of K-squares sintered at (a) 1280 °C and (b) 1320 °C.

Fig. 9, especially with water-based system. Because of this filling phase in grain boundaries, tapes made from BT 219-6 show generally higher sintered density as well as the abnormal grain growth at the lower temperature. With the solvent-based system, the onset temperature for abnormal grain growth is decreased approximately 40 °C with water-based systems in same sintering condition. This result can be explained with the Ba^{2+} leaching of the water-based system. According to Anderson et al.,[18] the leached Ba^{2+} ion enhanced the abnormal grain growth by redeposition onto the surface of the powder. They also mentioned that the type of binder was also found to affect the degree of abnormal grain growth during the sintering. To ensure the reliability of the MLCCs with 3 μm thick dielectric layers, more than five grains at each layer are required,[19] a

condition not possible with abnormal grain growth. Although we can control the grain size by changing sintering temperature or by adding sintering aids, sintering properties of $BaTiO_3$ is very important because more than 85 wt.% of X7R/Y5V MLCC is made of $BaTiO_3$ powder.

Fig. 10 shows the dielectric permittivity (Er) and dissipation factor (DF) measured at 1 kHz with 1 V_{rms}. The dielectric permittivities of the 1320 °C samples are lower than those of the 1280 °C. This finding correlates to the grain growth of the 1320 °C samples shown in Fig. 9. According to Kinoshita and Yamaji,[20] when $BaTiO_3$ particle size decreases from 53 to 1.1 μm, the cell polarizability increases due to the reduced tetragonal deformation. Consequently, the dielectric permittivity at room temperature increases. By decreasing the size from 0.8 to 0.2 μm, however, the dielectric permittivity also decreases because of the increased tetragonal deformation due to the high surface area to bulk ratio.[21] Therefore, a pure $BaTiO_3$ with a grain size of around 1 μm shows the highest dielectric permittivity. BT-8 samples sintered at 1280 °C exhibit a grain size of approximately 1 μm in this experiment. The DF is generally taken as an indicator of the quality of a MLCC. Most of the samples showed a dissipation factor of less than 5%, which is quite favorable for MLCC applications.

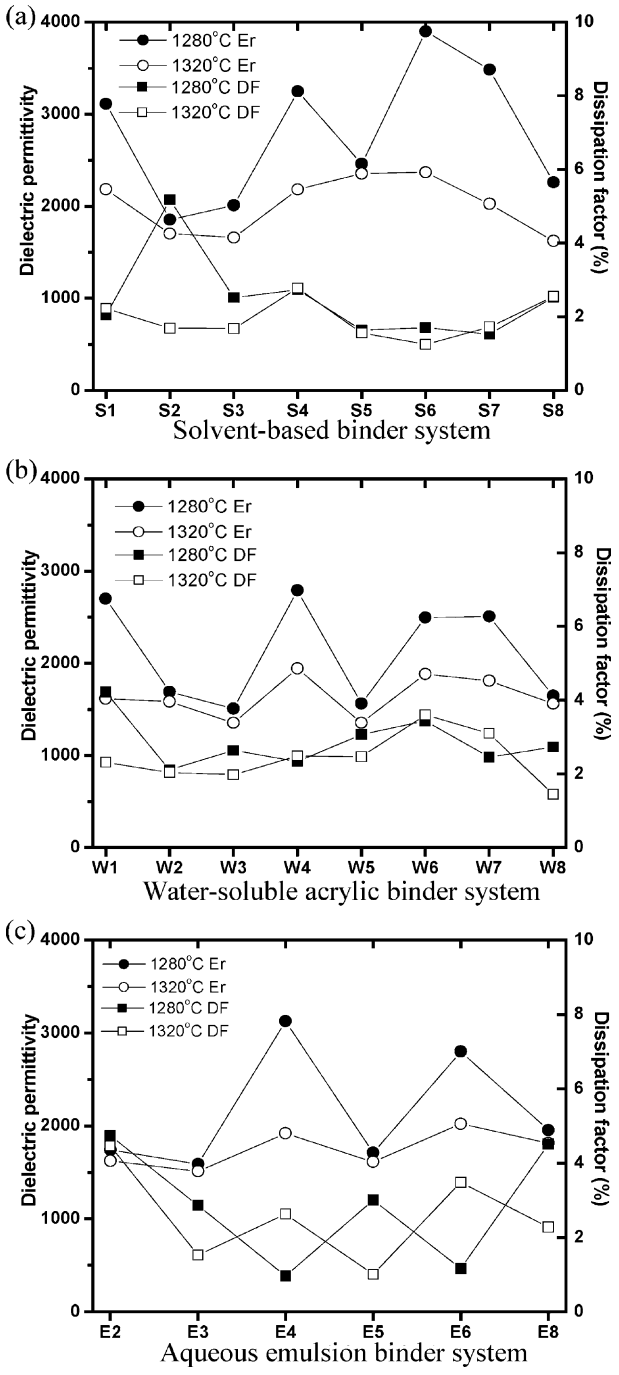

Fig. 10. Dielectric permittivity (Er) and dissipation factor (DF) measured at 1 kHz for three different systems which were sintered at 1280 and 1320 °C.

3.4. Optimization

For each output response, a model equation can be drawn with any number of input factors, so that we can decide the optimum condition easily based on that equation with the help of MINITAB. However, if there are many output responses as in this case, the optimization becomes difficult. Furthermore, in a practical sense, when one factor is changed to get an optimal response, it might worsen other responses. Therefore, we have tried to find the optimum condition among different experimental runs using a scorecard for each system.

The scorecard, modified from the traditional house of quality (HOQ) used in quality function deployment (QFD),[22–24] is shown in Table 3. This is a simple spreadsheet used to rank numerically all samples in relation to important output responses. The values in this table are based on the subjective interpretation of the experimental results. The upper part of this table is composed of 10 output responses considered important for the MLCC process, with the most important one receiving the highest number. The left side of the matrix consists of each sample name investigated as an experimental run. The numbers in the body of the matrix indicate the numerical effect rate of each sample on each output response. A higher score means a more favorable result for each output response. The rank column on the right was determined by multiplying each sample score by the corresponding weight at the top of the column and then adding these 10 products for each sample. Therefore, the sample with the highest value indicates the most desirable condition among eight experimental runs.

Based on these results, the most optimum experimental condition for solvent-based system is S7, made from BT-8 with B-98 polymer resin, a solvent/resin ratio of 10/1, and 10 wt.% binder resin with respect to the ceramic powder. The reason why this combination is the

Table 3
Scorecard used to select the optimal condition for three different systems

Output Responses	Dispersion	Slip viscosity	Air bubbles	Green density	Green morphology	Peel & Strength	Tacky	Sintered density	Permittivity	Dissipation factor		
Weight	7	3	7	8	4	5	5	9	7	7		
Sample	**Solvent-based binder system**										**Rank**	**% Rank**
S1	5	7	9	9	9	9	5	3	9	7	436	12.08%
S2	5	5	9	5	5	2	5	7	4	5	334	9.26%
S3	7	5	9	5	5	5	9	5	5	7	386	10.70%
S4	7	8	9	7	9	7	5	7	9	7	463	12.83%
S5	7	9	9	7	7	7	9	5	7	9	460	12.75%
S6	7	4	9	9	9	9	9	7	9	9	511	14.16%
S7	9	7	9	9	9	9	9	9	9	9	552	15.30%
S8	9	8	9	6	7	5	9	8	7	7	466	12.92%
Sample	**Water-soluble acrylic binder system**											
W1	9	9	7	9	9	9	9	3	9	7	476	14.90%
W2	9	7	5	5	3	3	5	7	5	9	372	11.65%
W3	9	5	7	9	7	5	5	7	5	9	438	13.71%
W4	7	9	5	3	3	7	9	5	9	9	398	12.46%
W5	9	5	5	5	7	5	5	7	5	7	378	11.83%
W6	9	9	7	5	3	7	9	5	9	7	428	13.40%
W7	9	5	5	5	9	5	5	5	9	9	410	12.84%
W8	3	5	7	3	3	3	3	5	5	9	294	9.20%
Sample	**Aqueous emulsion binder system**											
E2	5	5	5	5	3	3	9	5	5	5	312	13.82%
E3	9	5	5	9	5	7	9	7	5	5	418	18.51%
E4	5	5	7	5	3	5	9	3	9	9	374	16.56%
E5	9	7	7	9	7	7	9	9	5	5	464	20.55%
E6	5	7	3	5	3	5	9	5	9	9	370	16.39%
E8	5	5	5	3	3	5	9	5	7	5	320	14.17%

most favorable are: (1) the fine $BaTiO_3$ particle size and the uniform size distribution yielding favorable green properties, (2) the higher T_g value of B-98 resin with lower molecular weight for the high green strength and low slip viscosity, (3) the higher solvent to resin ratio yielding a desirable slip viscosity and dispersion, (4) the optimum amount of binder for easy processing, and (5) the good sintered density yielding optimum dielectric properties.

The most optimum condition for water-soluble system is W1, made from BT-8 with m-PMMA dispersant, a water/resin ratio of 8/1, and an 8 wt.% binder resin with respect to the ceramic powder. However, we need to increase the sintered density by modifying the sintering profile or by adding sintering aids with these conditions. The reasons are: (1) the fine $BaTiO_3$ particle size and the uniform size distribution yielding favorable green mechanical strength and the sintered properties, (2) the higher degree of dispersion and better green microstructure with m-PMMA dispersant, and (3) the smaller water/resin ratio and the amount of binder added yielding a desirable slip viscosity and long-term stability.

For emulsion system, the optimum condition is E5, made from BT 219-6 with PApA-Na dispersant, a water/resin ratio of 6/1, and a 12 wt.% binder resin. The reasons are: (1) BT 219-6 ceramic powder with chemical compatibility with emulsion binder and higher sintered density (2) PApA-Na dispersant with the better green microstructure and strength, and (3) the smaller water/resin ratio and the higher binder amount added yielding a desirable slip viscosity and long-term stability. Compared to other two systems both of which show the optimum condition with fine BT-8 ceramic powder,[24,25] selection for the optimum condition is restricted at this time due to the chemical reaction between BT-8 and emulsion binder system. Finding a good chemical formulation, which is compatible with BT-8 ceramic powder can result a different optimum condition because a fine powder with uniform size distribution shows much favorable results in terms of the mechanical strength,

green morphology, uniform sintered microstructure, and dielectric properties based on other systems.

Among the best for each system, S7 of the solvent-based system shows the highest score, which means the most favorable condition for the application as shown in Table 3. However, some of water-based systems including W1 and E5 with comparable score deserve their possibility for MLCC application due to reduced health and environmental hazards with lower cost compared with the solvent-based system.

4. Conclusions

The results presented above enable the following conclusions to be drawn:

1. All slips prepared in this experiment showed adequate properties for tape casting except for E1 and E7 samples due to the gelation during the slip preparation.
2. The green properties of solvent-based system depended significantly on the ceramic powder, while dispersant was the most significant factor for those of two water-based systems.
3. The modified PMMA was a more efficient dispersant than APA for water-soluble acrylic binder system, and PApA-Na than APA for emulsion system.
4. Ceramic powder was the most significant factor for the sintered properties such as microstructure, density and dielectric permittivity for all three systems.
5. Optimization using a scorecard showed that BT-8 powder with B-98 resin at a 10/1 solvent to resin ratio and 10 wt.% loading was the best slip condition for solvent-based system. BT-8 with KD-6 dispersant at 8/1 water to resin ratio and 8 wt.% binder loading was the optimum condition for the water-soluble acrylic binder system. BT 219-6 with PApA-Na dispersant at 6/1 water to resin ratio and 12 wt.% of binder loading was the optimum condition with emulsion type binder system for MLCC application.

Acknowledgements

This research is based upon the work supported by the National Science Foundation under Grant No. DMR-9731769. Any opinions, findings and conclusions, or recommendations expressed here are those of the authors and do not necessarily reflect the views of the National Science Foundation.

References

1. Yoon, D. H. and Lee, B. I., $BaTiO_3$ properties and powder characteristics for ceramic capacitors. *J. Ceram. Proc. Res.*, 2002, **3**(2), 41–47.
2. Robinson, G. K., *Practical Strategies for Experimenting*. John Wiley & Sons, New York, 2000.
3. Montgomery, D. C., *Design and Analysis of Experiments*, 3rd edn. John Wiley & Sons, New York, 1991.
4. Blackman, K., Slilaty, R. M. and Lewis, J. A., Competitive adsorption phenomena in nonaqueous tape casting suspensions. *J. Am. Ceram. Soc.*, 2001, **84**(11), 2501–2506.
5. Lewis, J. A., Binder removal from ceramics. *Annu. Rev. Mater. Sci.*, 1997, **27**, 147–173.
6. Wesselmann, M., *Polymer Innovations*, San Marcos, CA (private communication).
7. Yoon, D. H. and Lee, B. I., Barium ion leaching from barium titanate powder in water. *J. Mat. Sci.: Mat. Electro.*, 2003, **14**, 165–169.
8. Wang, X., *Synthesis and Dispersion of Nanocrystalline Barium Titanate Particles*, PhD dissertation, Clemson University, Clemson, SC, 2002.
9. Bierwagen, G. P. and Saunders, T. E., Studies of the effects on particle size distribution on the packing efficiency of particles. *Powder Tech.*, 1974, **10**, 111–119.
10. Sohn, H. Y. and Moreland, C., The effect of particle size distribution on packing density. *Can. J. Chem. Eng.*, 1968, **46**, 162–167.
11. Moreno, R., The role of slip additives in tape-casting technology: Part I—solvents and dispersants. *Am. Ceram. Soc. Bull.*, 1992, **71**(10), 1521–1531.
12. Onoda, G. Y. Jr, Theoretical strength of dried green bodies with organic binders. *J. Am. Ceram. Soc.*, 1976, **59**, 236–239.
13. Nies, C. W. and Messing, G. L., Effect of glass-transition temperature of polyethylene glycol-plasticized polyvinyl alcohol on granular compaction. *J. Am. Ceram. Soc.*, 1984, **67**, 301–304.
14. Pritchard, J. G., *Polyvinyl Alcohol*. Gordon and Breach, New York, 1970.
15. Herard, C., Faivre, A. and Lemaitre, J., Surface decontamination treatments of undoped $BaTiO_3$—Part II: influence of sintering. *J. Eur. Ceram. Soc.*, 1995, **15**, 145–153.
16. Page, C. H., Thombare, C. H., Varadarojan, V., Borkar, S. A. and Chatterjee, A. K., Characteristics and sintering behavior of barium titanate powders obtained by various synthetic routes. *Solid State Phenomena*, 1992, **25 & 26**, 317–326.
17. Levin, E. M., Robbins, C. R. and McMurdie, H. F., *Phase Diagrams for Ceramist*. American Ceramic Society, Columbus OH, 1964.
18. Anderson, D. A., Adair, J. H., Miller, D., Biggers, J. V. and Shrout, T. R., Surface chemistry effects on ceramic processing of $BaTiO_3$ powder. In *Ceramic Powder Science II. Ceramic Transactions, Vol. 1*, ed. G. L. Messing, E. R. Fuller Jr and H. Hausner. American Ceramic Society, OH, 1988, pp. 485–492.
19. Sakabe, Y., MLCs technologies of today and future. In *Proceedings of the 9th US-Japan Seminar on Dielectric and Piezoelectric Ceramics*. Japan, 1999, pp. 1–6.
20. Kinoshita, K. and Yamaji, A., Grain-size effects on dielectric properties in barium titanate ceramics. *J. Appl. Phys.*, 1976, **47**(1), 371–373.
21. Herczog, A., Application of glass-ceramics for electronic components and circuits. *IEEE Trans., Parts, Hybrids, Packag.*, 1973, **PHP-9**(4), 247–256.
22. Halog, A., Schultmann, F. and Rentz, O., Using quality function deployment for technique selection for optimum environmental performance improvement. *J. Clean. Prod.*, 2001, **9**, 387–394.
23. Chan, L. K. and Wu, M. L., Quality function deployment: a literature review. *Eur. J. Operational Res.*, 2002, **143**(3), 463–497.
24. Park, T. and Kim, K. J., Determination of an optimal set of design requirements using house of quality. *J. Operational Manag.*, 1998, **16**, 569–581.